Spatial dynamics in Arctic bacterioplankton community densities are strongly linked to distinct physical and biological processes (Fram Strait, 79°N)

Magda G. Cardozo Mino[1,2*#], Eduard Fadeev [1,2,3#], Verena Salman-Carvalho[1,2,4], Antje Boetius[1,2]

[1]Max Planck Institute for Marine Microbiology, D-28359 Bremen, Germany

[2]Alfred Wegener Institute, Helmholtz Center for Polar and Marine Research, D-27570 Bremerhaven, Germany

[3]Current affiliation: Department of Functional and Evolutionary Ecology, University of Vienna, A-1090 Vienna, Austria

[4]Current affiliation: Department of Microbiology, University of Massachusetts, Morrill Science Center IVN, MA 01003, Amherst, USA

# equal contribution

*** Correspondence:**
Magda G. Cardozo
mcardozo@mpi-bremen.de

Keywords: Arctic Ocean, Fram Strait, bacterioplankton, CARD-FISH, water column

Abstract

The Arctic is impacted by climate warming faster than any other oceanic region on Earth. Assessing the baseline of microbial communities in this rapidly changing ecosystem is vital for understanding the imminent implications of Arctic warming and sea ice retreat on ecosystem functioning. Using CARD-FISH and semi-automated counting, we quantified 14 ecologically relevant taxonomic groups of bacterioplankton (*Bacteria* and *Archaea*) from surface (0– 30 m) down to deep waters (2500 m) in summerly ice-covered and ice-free regions of the Fram Strait, the main gateway for Atlantic inflow into the Arctic Ocean. Cell abundances of the bacterioplankton communities in surface waters varied from 10^5 cells mL^{-1} in ice-covered region to 10^6 cells mL^{-1} in the ice-free region and were overall driven by variations in phytoplankton bloom conditions across the Strait. In surface waters the bacterial classes *Bacteroidia* and *Gammaproteobacteria* showed several-fold higher cell abundances under late phytoplankton bloom conditions of the ice-free regions. Other taxonomic groups, such as the *Rhodobacteraceae*, revealed a distinct association of cell abundances with the surface Atlantic waters. With depth (> 500 m) the total cell abundances of the bacterioplankton communities decreased by one to two orders of magnitude, while largely unknown taxonomic groups (e.g., SAR324 and SAR202 clades) maintained constant cell abundances throughout the entire water column (10^3 cells mL^{-1}). This suggests that some enigmatic taxonomic groups may occupy a specific ecological niche in the entire water column. Our results provide the first quantitative spatial variations assessment of bacterioplankton in summerly ice-covered and ice-free Arctic water column, and suggest that further shift towards ice-free Arctic summers with longer phytoplankton blooms can lead to major changes in the associated standing stock of the bacterioplankton communities.

1 Introduction

Atmospheric and oceanic warming has a substantial impact on the Arctic Ocean already today (Dobricic et al., 2016; Sun et al., 2016; Dai et al., 2019). The strong decline in sea ice coverage (Peng and Meier, 2018; Dai et al., 2019) and the increasing heat transfer by the Atlantic water inflow (Beszczynska-Möller et al., 2012; Rudels et al., 2013; Walczowski et al., 2017) will affect stratification of the water column and can lead to an increased vertical mixing of the deep Atlantic core water, a process also termed "Atlantification" (Polyakov et al., 2017). The main inflow of Atlantic water into the Arctic Ocean occurs through the Fram Strait (Beszczynska-Möller et al., 2011), making it a sentinel region for observing the ongoing changes in the Arctic marine ecosystem (Soltwedel et al., 2005, 2016). The Fram Strait is also the main deep-water gateway between the Atlantic and the Arctic Oceans. It is a spatially dynamic region (Wekerle et al., 2017), with two distinct hydrographic regimes: the West Spitsbergen Current (WSC) that carries relatively warm and saline Atlantic water northwards along the Svalbard shelf (Beszczynska-Möller et al., 2012; von Appen et al., 2015), and the East Greenland Current (EGC) that transports cold polar water and sea ice southwards from the Arctic Ocean along the ice-covered Greenland shelf (de Steur et al., 2009).

Sea ice conditions have a strong impact on the seasonal ecological dynamics in the Arctic Ocean (Wassmann and Reigstad, 2011), and sea-ice algae can make up a significant proportion of the annual productivity (Leu et al., 2011; Boetius et al., 2013; Fernández-Méndez et al., 2014). However, the presence of sea ice and variations in its snow cover can repress the seasonal phytoplankton bloom in the water column through light limitation (Mundy et al., 2005; Leu et al., 2011), or change its timing, e.g. by increasing stratification of the surface waters once the ice melts (Korhonen et al., 2013). Previous summer observations in Fram Strait already suggested that total cell abundances and productivity of bacterioplankton communities in surface waters is driven by environmental parameters associated with phytoplankton bloom dynamics (Fadeev et al., 2018), such as the availability and composition of organic matter (Piontek et al., 2015; Engel et al., 2019), with differences between ice-covered and ice-free regions (Piontek et al., 2014; Fadeev et al., 2018).

Long-term summer observations in the region, conducted in the framework of the Long-Term Ecological Research (LTER) site HAUSGARTEN, revealed strong ecological variations associated with the Atlantic Meridional Overturning Circulation (AMOC)(Soltwedel et al., 2016). Warming events during the past decades influenced seasonal phytoplankton blooms by causing a slow but continuous increase in biomass, and a shift from diatom- to flagellate-dominated communities (Nöthig et al., 2015; Engel et al., 2017; Basedow et al., 2018). It has been also observed that phytoplankton blooms of recent years show an increasing partitioning of the produced organic carbon into the dissolved phase (Engel et al., 2019), which may result in a more active microbial loop in the upper ocean and less export of particulate matter (Vernet et al., 2017). In times of a rapidly changing Arctic ecosystem, investigating the structure and the dynamics of bacterioplankton communities remains a key component to understand the ongoing changes on this environment. However, so far, an assessment of associated responses of the key bacterial taxa responsible for increased recycling is missing, especially with regard to shifts in standing stocks.

To date, the majority of Arctic bacterioplankton studies are performed using high-throughput sequencing of the 16S rRNA gene, which cannot directly be converted to absolute standing stock abundances of specific taxonomic groups due to PCR and other quantitative biases (Gloor et al., 2017; Kumar et al., 2018; Piwosz et al., 2020). Here we used semi-automatic CAtalyzed Reporter Deposition-Fluorescence In Situ Hybridization (CARD-FISH; (Pernthaler et al., 2002)), power of which lies in the ability to acquire absolute abundance of the targeted taxonomic groups free of

compositional effect (Amann et al., 1990). While specific taxonomic groups can be targeted and quantified, also the positive hybridization signal provides additional information that the analyzed cells were alive and active before fixation (Amann et al., 1990; DeLong et al., 1999). Automatization of the microscopic examination and counting procedure allowed us to reach a high-throughput standard (Schattenhofer et al., 2009; Teeling et al., 2012; Bižić-Ionescu et al., 2015; Bennke et al., 2016). Using this technique, we quantified cell abundances of 14 taxonomic groups in 44 samples, collected at 4 different water layers from surface (15 - 30 m) to the deep ocean (2500 m) in both ice-free and ice-covered regions of the Fram Strait. The main objective of this study was to assess the standing stocks of key taxonomic groups in summerly Arctic bacterioplankton across the Strait. Using the high-throughput data of bacterioplankton cell abundances we tested previously established hypotheses that: 1) in surface waters the abundance of various taxonomic groups is associated with phytoplankton bloom conditions and is linked to the abundance of specific phytoplankton populations (Fadeev et al., 2018); 2) with an increasing depth the differences between bacterioplankton communities in ice-covered and ice-free regions decrease, and various taxonomic groups that are associated with winterly bacterioplankton dominate the deep sea communities.

2 Results and Discussion

2.1 Bacterioplankton communities strongly change in cell abundance and composition with depth

We investigated a total of 44 water samples from 11 stations that represented different hydrographic and biogeochemical conditions across Fram Strait (Figure 1; Table S1). At each station, 4 different water layers were targeted: the surface mixed layer (0 – 30 m), epipelagic waters (100 m), deep mesopelagic waters (500 – 1000 m), and bathypelagic waters (1200 – 2500 m; Table S2). Based on the known hydrography of the Fram Strait (Rudels et al., 2013), and observed sea-ice conditions, the sampled stations were grouped into three distinct regions (Figure 1): the eastern ice-free region associated with the WSC (Beszczynska-Möller et al., 2012), the western ice-covered region associated with the EGC (de Steur et al., 2009), and the partially ice-covered region in the north-east that is associated with the highly productive marginal ice zone (further addressed as North; i.e. "N") (Hebbeln and Wefer, 1991; Perrette et al., 2011). At the time of sampling in June-July 2016, chlorophyll *a* concentrations showed a developed phytoplankton bloom across the Strait (Table S1). Thus, fitting the interannual trend of summerly phytoplankton bloom conditions in the western ice-covered EGC and the eastern ice-free WSC (Nöthig et al., 2015; Fadeev et al., 2018).

We found that in all three regions, total cell abundances of the entire bacterioplankton community were highest at the surface with 10^5 – 10^6 cells mL^{-1}, and significantly decreased with depth down to 10^4 cells mL^{-1} at meso- and bathypelagic depths (Figure 2a; Kruskal-Wallis test; Chi square = 554.39, df = 3, p-value < 0.01). Members of the domain *Bacteria* dominated the communities throughout the entire water column, with highest cell abundances in surface waters (10^5 – 10^6 cells mL^{-1}), and significantly lower abundances at depth (10^4 cells mL^{-1}; Figure 2b; Kruskal-Wallis test; Chi square = 35.27, df = 3, p-value < 0.01). Archaeal cells had overall an order of magnitude lower abundance than bacterial cells throughout the entire water column, ranging from 10^4 cells mL^{-1} at the surface down to 10^3 cells mL^{-1} in the bathypelagic waters (Figure 2c). However, unlike *Bacteria*, archaeal communities doubled their absolute cell abundances from the surface to 100 m depth (reaching up to 6×10^4 cells mL^{-1}), followed by a significant decrease in cell abundance at meso- and bathypelagic depths (Kruskal-Wallis test; Chi square = 29.04, df = 3, p-value < 0.01). This pattern fits the known global trend of archaeal enrichment in epipelagic waters (Karner et al., 2001; Herndl et al., 2005; Kirchman et al., 2007; Varela et al., 2008; Schattenhofer et al., 2009) and was also

observed in other regions of the Arctic Ocean (Amano-Sato et al., 2013). Altogether, the observed cell numbers in the surface waters were well within the range of previous observations in the Fram Strait waters (Piontek et al., 2014; Fadeev et al., 2018; Engel et al., 2019). Below the upper 100 m the observed bacterioplankton cell abundances were lower than the ones previously reported from the eastern Fram Strait by Quero et al. (2019). The discrepancy might be associated with methodological differences in the duration of cell staining incubation and the usage of automated vs. manual counting approach. Nevertheless, both studies showed a similar pattern of a strong decrease in bacterioplankton cell abundances with depth, which also matches observations in other oceanic regions (Karner et al., 2001; Church et al., 2003; Teira et al., 2004; Schattenhofer et al., 2009; Dobal-Amador et al., 2016).

In the surface waters, around 60% of the DAPI-stained total bacterioplankton community was covered by the *Bacteria*-specific probes in all stations (Table S2). At depth (>100 m) the total coverage of the *Bacteria*-specific probes strongly decreased to 16-40% of DAPI-stained cells (ANOVA; $F_3 = 15.39$, $p < 0.01$; Table S2). Similar decrease in detectability of the domain-specific probes (EUB388I-III) was previously observed in other bacterioplankton microscopy studies (Karner et al., 2001; Herndl et al., 2005; Varela et al., 2008; Schattenhofer et al., 2009), and is potentially explained by a decrease in ribosomal nucleic acids within the bacterial cells (i.e. lower activity) towards the oligotrophic depths, or an increasing fraction of microbial cells that are not captured by the currently existing probes (Hewson et al., 2006; Sogin et al., 2006; Galand et al., 2009a; Agogué et al., 2011; Salazar et al., 2016).

Interestingly, the *Archaea*-specific probe showed a different trend. In surface waters, the coverage of the probe was higher in the EG stations (8% of DAPI-stained cells), compared to HG and N stations (1-2% of DAPI-stained cells; Table S2). At depth (>100 m), the coverage of the *Archaea*-specific probe increased significantly to 13-17% of DAPI-stained cells (ANOVA; $F_3 = 34.31$, $p < 0.01$), which implies an increase in relative abundance with depth (Müller et al., 2018b). Taken together, our findings confirm previously observed higher abundance of *Archaea* in bacterioplankton communities of ice-covered waters (Wilson et al., 2017; Müller et al., 2018b), and correspond to the globally observed trend of an increasing archaeal importance at depth (Herndl et al., 2005; Teira et al., 2006; Galand et al., 2009b)

2.2 Surface water bacterioplankton communities are affected by distinct phytoplankton bloom conditions

Phytoplankton blooms in surface waters lead to an increasing cell abundance of heterotrophic bacteria that are specialized on degradation of organic matter from algal exudates and phytodetritus (Buchan et al., 2014; Teeling et al., 2016). Previous observations in the Fram Strait, acquired using high-throughput sequencing of the 16S rRNA gene, revealed a strong influence of the summerly phytoplankton bloom conditions on the bacterioplankton communities (Wilson et al., 2017; Müller et al., 2018a), differing between the ice-covered and ice-free regions of the Strait (Fadeev et al., 2018).During the sampling period, distinct phytoplankton bloom communities in surface waters across the Strait were observed, with a *Phaeocystis*-dominated bloom in the ice-free HG stations, a diatom-dominated bloom in the ice-covered EG stations, and a mixed diatoms and *Phaeocystis* populations bloom in the ice-margin stations N (data not included). Surface water total bacterioplankton communities showed significantly higher cell abundances in the HG and N stations (13-21 $\times 10^5$ cells mL^{-1}), compared to the EG stations (0.5-2 $\times 10^5$ cells mL^{-1}; Kruskal-Wallis test; Chi square = 81.85, df = 2, p-value < 0.01). The communities were dominated by bacterial cells that comprised 8-11 $\times 10^5$ cells mL^{-1} in the HG and N stations, and 2 $\times 10^5$ cells mL^{-1} in the EG stations.

Within the bacterial communities, a group of bacterial classes that are functionally associated with phytoplankton blooms in the region (*Bacteroidia*, *Gammaproteobacteria*, and the phylum *Verrucomicrobia*) (Fadeev et al., 2018) showed together several-fold higher cell abundances in the HG and N stations (2.3-10 × 10^5 cells mL^{-1}), compared to the EG stations (0.5-1.5 × 10^5 cells mL^{-1}). Jointly comprising up to 50% of the bacterioplankton communities (Table 1). However, other taxonomic groups, which were previously known to be associated with the polar water masses and winter communities in the Fram Strait (e.g., the class *Deltaproteobacteria* and the *Thaumarchaeota*) (Wilson et al., 2017; Fadeev et al., 2018; Müller et al., 2018b), showed higher cell abundances in the ice-covered EG stations, compared to the ice-free HG and ice-margin N stations (Table 1). Thus, suggesting that the cell abundances of different taxonomic groups may be associated with different environmental conditions (i.e., phytoplankton bloom vs. water masses)

To test whether the observed differences in cell abundances are a result of distinct biological conditions (i.e., phytoplankton bloom) or distinct physical conditions (Atlantic vs. Arctic water masses) we conducted specific correlation tests between the cell abundances of different taxonomic groups and various environmental parameters. For that purpose, we defined physical characteristics of the water as a proxy for the distinct surface water masses (Rudels et al., 2013). We identified that the cell abundances of the phylum *Verrucomicrobia* and the order *Opitutales* within it, as well as the SAR11 clade and the *Rhodobacteraceae* family (both within the class *Alphaproteobacteria*), showed strong positive correlation with statistical significance to water temperature (Pearson's correlation; $r > 0.5$, p-value < 0.05; Table S3), suggesting a potential association with the warmer Atlantic waters of the eastern Fram Strait. The phylum *Verrucomicrobia* has been previously shown to be a major polysaccharide-degrading bacterial taxonomic group in Svalbard fjords (Cardman et al., 2014), and therefore may also be associated with the outflow from the Svalbard fjords into the Atlantic waters of the WSC (Cottier et al., 2005). The SAR11 clade and the family *Rhodobacteraceae*, both have been previously shown to correlate with temperature at high latitudes (Giebel et al., 2011; Tada et al., 2013), and are known to have distinct phylotypes in water masses with different temperatures (Selje et al., 2004; Sperling et al., 2012; Giovannoni, 2017). However, the family *Rhodobacteraceae* is also known for their broad abilities in utilizing various organic compounds (Buchan et al., 2014; Luo and Moran, 2014), and thus one cannot rule out that their higher cell densities in warmer waters of the WSC and N regions are associated with the developed phytoplankton bloom in these regions. In addition, the SAR324 clade (class *Deltaproteobacteria*) showed strong positive correlation with statistical significance to salinity (Pearson's correlation; $r > 0.5$, p-value < 0.05; Table S3). During summer with increasing melt of sea ice, a low-salinity water layer is formed in surface waters. The strong stratification of this water layer enhances the development of the phytoplankton bloom (Fadeev et al., 2018). Thus, the correlation of these taxonomic groups with salinity rather suggests that their cell abundances are lower in surface waters with strong phytoplankton bloom (i.e., in WSC and N regions).

Because distinct water masses in the region differ not only in their physical characteristics but also in their inorganic nutrient budgets (Wilson and Wallace, 1990), we disentangled the effect of physical and biological parameters by calculating the seasonal net consumption of inorganic nutrients as the proxy for phytoplankton bloom state (Table S2) (Fadeev et al., 2018). Consumed nitrate (ΔNO_3) and phosphate (ΔPO_4) revealed a very strong positive correlation between them with statistical significance (Pearson's correlation; $r = 0.86$, p-value < 0.05). These two nutrients are required for phytoplankton growth in a constant ratio ('The Redfield ratio'), and thus the strong correlation between their consumption is expected. The consumed silica (ΔSiO_3), which is used only by diatoms, did not show significant correlation to ΔPO_4 and ΔNO_3, which further supports that there are different phytoplankton populations across the Strait (i.e., diatoms vs. *Phaeocystis*). Phytoplankton

bloom associated environmental parameters (chlorophyll *a* concentration and the consumed inorganic nutrients) revealed weaker relationships with cell abundances of the different taxonomic groups (Table S3). This might be explained by smaller differences in these parameters between the regions, due to an overall ongoing phytoplankton bloom across the entire Strait (Table S2). The class *Gammaproteobacteria* showed strong correlation with statistical significance to ΔPO_4 (Pearson's correlation; $r = 0.74$, p-value < 0.05; Table S3). The correlation suggests a strong uptake of phosphate by *Gammaproteobacteria* that confirms their strong growth and high activity during phytoplankton blooms (Joint et al., 2002; Buchan et al., 2014).

The complexity of surface waters in Fram Strait, with different ice-coverage, the opposing water regimes (Atlantic and Polar water masses) along with complex mesoscale mixing events (Wekerle et al., 2017), and a dynamic ice-melt water layer, challenges the identification of specific associations between microbial cell abundances and environmental parameters. Nevertheless, our results showed that elevated cell abundances of some taxonomic groups (e.g., *Gammaproteobacteria*) are more likely to be associated with the phytoplankton bloom conditions observed at the site (e.g. through a link with algal exudates and nutrients as main source for growth) (Tada et al., 2011; Teeling et al., 2012), while other taxonomic groups (e.g., SAR11 clade) might be more influenced by the distinct Arctic water masses (Kraemer et al., 2020).

2.3 Enigmatic microbial lineages increase in cell abundance towards the deep ocean

The deep waters of the Fram Strait basin (> 500 m) have a rather homogeneous hydrography (von Appen et al., 2015), and are less affected by the seasonal dynamics governing the surface layers (Wilson et al., 2017). Previous molecular observations of the deep waters bacterioplankton communities showed high sequence abundance of largely unknown taxonomic groups, such as the SAR202 (class *Dehalococcoidia*), SAR324 (class *Deltaproteobacteria*), and SAR406 (phylum *Marinimicrobia*) (Wilson et al., 2017; Quero et al., 2019). There was also higher archaeal sequence abundance at depth, with the class *Nitrososphaeria* reaching up to 15% of the sequences in mesopelagic waters (> 200 m) (Wilson et al., 2017; Müller et al., 2018b). However, it has been also recently shown that in ice-covered regions of the Strait surface dominant taxonomic groups, such as *Gammaproteobacteria* and *Nitrososphaeria*, are exported via fast-sinking aggregates from surface to the deep ocean (> 1000 m), where they may realize an ecological niche. We observed that in all regions the total cell abundances of the bacterioplankton communities were in the range of 10^4 cells mL^{-1} in both meso- and bathypelagic waters (Figure 2), matching previous observations in other regions of the Arctic Ocean (Wells and Deming, 2003; Wells et al., 2006). Bacterial taxonomic groups that dominated the surface water communities (e.g., *Bacteroidetes*, *Gammaproteobacteria* and *Verrucomicrobia*), in both ice-free and ice-covered regions of the Strait, decreased by two orders of magnitude in their cell abundances at meso- and bathypelagic depths (Kruskal-Wallis test; p-value < 0.01; Table 2). This trend strongly correlated along the water column with the total bacterioplankton cell abundances (Pearson's correlation; $r > 0.8$, p-value < 0.05; Figure S1). In contrast, other bacterial groups, such as the SAR202 clade (class *Dehalococcoidia*) and SAR324 (class *Deltaproteobacteria*), proportionally decreased in cell abundances with depth, and maintained overall constant cell abundances of ca. 0.5×10^4 cells mL^{-1} throughout the entire water column (Table 2). Previous molecular studies of bacterioplankton communities in Fram Strait suggested a proportional increase of these largely understudied bacterial lineages in the deep ocean (Wilson et al., 2017). The cell abundances that are presented here indicate that their increasing proportional abundance at depth is due to stronger decrease in the cell abundances of other groups (Table 2; Table S4). Very little is currently known about these two taxonomic groups, but previous genetic observations suggest that they possess distinct metabolic capabilities, and may be involved in the

degradation of recalcitrant organic matter (SAR202; (Landry et al., 2017; Colatriano et al., 2018; Saw et al., 2020); or in sulfur oxidation (SAR324; (Swan et al., 2011; Sheik et al., 2014), which is however a highly unlikely energy source for the fully oxidized, oligotrophic polar waters. Their homogeneous distribution from the stratified surface to the homogenous deep ocean of the Fram Strait suggests that these enigmatic bacterial groups fulfil an ecological niche that exists in the entire water column, and thus may have unique roles in oceanic nutrient cycling.

Proportionally, the decrease with depth of archaeal cell abundances was less than of *Bacteria* (Table S4). The *Thaumarchaeota* phylum strongly correlated with the pattern of the archaeal cell abundances (Pearson's correlation; $r = 0.76$, p-value < 0.05; Figure S1), with a two-fold increase in cell abundances from surface to epipelagic depth (100 m), followed by a substantial decrease towards meso- and bathypelagic waters (Table S4). This general trend matches deep ocean observations in previous quantitative studies of other oceanic regions (Karner et al., 2001; Church et al., 2003; Herndl et al., 2005). It has been shown in molecular studies that *Thaumarchaeota* comprise a large proportion of the bacterioplankton communities in the Fram Strait, especially in the epipelagic waters (Wilson et al., 2017; Müller et al., 2018b). In our study, the *Thaumarchaeota* exhibited the highest cell abundances at 100 m in the ice-free HG and ice-margin N stations (3×10^4 cells mL^{-1}), where they comprised half of the total archaeal community (Table S2). The strong absolute decrease of *Thaumarchaeota* cell abundances towards the meso- and bathypelagic waters may represent a decrease in activity with depth (Herndl et al., 2005; Kirchman et al., 2007; Alonso-Saez et al., 2012) and thus lower detection of the cells. Alternatively, the relative decrease within the total archaeal cells may suggest that other pelagic archaeal groups, such as the *Euryarchaeota*, increase in abundance at depth (Galand et al., 2010).

3 Conclusions

Using state-of-the-art semi-automatic microscopy counting, we quantified the absolute cell abundance of 14 key taxonomic groups in summer bacterioplankton communities of the Fram Strait. Our observations covered both the ice-free and the ice-covered regions of the Strait, which at the time of sampling were characterized by different seasonal phytoplankton bloom conditions. Our results showed that in surface waters, abundance of some taxonomic groups (e.g., *Rhodobacteraceae*) was to certain extent related to the distinct water masses of the Strait. However, in general the abundance of different taxonomic groups was strongly positively (e.g., *Gammaproteobacteria*) and negatively (e.g., SAR324 clade) associated to the progressing states of the seasonal phytoplankton bloom across the Strait**.** Based on our observations, we postulate that summer surface bacterioplankton communities in Arctic waters are shaped mostly by the phytoplankton bloom rather than the distinct water masses they are associated with. This suggests that currently predicted longer seasonal phytoplankton blooms, as well as the increasing Atlantic influence on the Arctic Ocean (i.e., 'Atlantification'), may have a strong impact on the biogeographical distribution of certain bacterioplankton taxonomic groups in the surface Arctic waters. This study also provides the first extensive quantitative overview of bacterioplankton communities in the deep Arctic water column (> 500 m). We showed that at depth, largely unknown taxonomic groups, such as the SAR202 clade, maintained similar abundance throughout the entire water column (2500 m depth), where other taxa decline by severalfold. This observation suggests that despite their low abundance, some taxonomic groups may potentially realize a unique ecological niche throughout the entire water column. Altogether, our results on cell abundances of ecologically relevant taxonomic bacterioplankton groups expanded previous molecular observations in the Fram Strait and provided new insights into the quantitative dynamics of pelagic bacterioplankton communities from surface to the deep waters of the Arctic Ocean.

4 Materials and Methods

4.1 Sampling and environmental data collection

Sampling was carried out during the RV Polarstern expedition PS99.2 to the Long-Term Ecological Research (LTER) site HAUSGARTEN in Fram Strait (June 24th – July 16th, 2016). Sampling was carried out with 12 L Niskin bottles mounted on a CTD rosette (Sea-Bird Electronics Inc. SBE 911 plus probe) equipped with temperature and conductivity sensors, a pressure sensor, altimeter, and a chlorophyll fluorometer. On board, the samples were fixed with formalin in a final concentration of 2% for 10 – 12 hours, then filtered onto 0.2 µm polycarbonate Nucleopore Track-Etched filters (Whatman, Buckinghamshire, UK), and stored at -20°C for further analysis.

Hydrographic data of the seawater including temperature and salinity were retrieved from PANGAEA (Tippenhauer et al., 2017), along with measured chlorophyll *a* concentrations (Nöthig et al., 2018) (Table S1).

4.2 Catalyzed reporter deposition-fluorescence in situ hybridization (CARD-FISH)

We quantified absolute cell abundances of 14 key bacterioplankton groups (Table S5), based on their relatively high sequence abundance and recurrences in previous molecular studies of Arctic waters (Bowman et al., 2012; Wilson et al., 2017; Müller et al., 2018b). CARD-FISH was applied based on the protocol established by (Pernthaler et al., 2002), using horseradish-peroxidase (HRP)–labelled oligonucleotide probes (Biomers.net, Ulm, Germany; Table S2). All probes were checked for specificity and coverage of their target groups against the SILVA database release 132 (Quast et al., 2012). All filters were embedded in 0.2 % low-gelling-point agarose, and treated with 10 mg mL^{-1} lysozyme solution (Sigma-Aldrich Chemie GmbH, Hamburg, Germany) for 1 h at 37°C. Filters for enumerating *Archaea* and *Thaumarchaeota* were treated for an additional 30 min in 36 U mL^{-1} achromopeptidase (Sigma-Aldrich Chemie GmbH, Hamburg, Germany) and 15 µg mL^{-1} proteinase K at 37°C. Subsequently, endogenous peroxidases were inactivated by submerging the filter pieces in 0.15 % H_2O_2 in methanol for 30 min, before rinsing in Milli-Q water and dehydration in 96 % ethanol. Then, the filters were covered in hybridization buffer and a probe concentration of 0.2 ng μL^{-1}. Hybridization was performed at 46°C for 2.5 h, followed by washing in pre-warmed washing buffer at 48°C for 10 min, and 15 min in 1x PBS. Signal amplification was carried out for 45 min at 46°C with amplification buffer containing either tyramide-bound Alexa 488 (1 µg/mL) or Alexa 594 (0.33 µg mL^{-1}). Afterwards, the cells were counterstained in 1 µg/mL DAPI (4′,6-diamidino-2-phenylindole; Thermo Fisher Scientific GmbH, Bremen, Germany) for 10 min at 46°C. After rinsing with Milli-Q water and 96 % ethanol, the filter pieces were embedded in a 4:1 mix of Citifluor (Citifluor Ltd, London, United Kingdom) and Vectashield (Vector Laboratories, Inc., Burlingame, United States), and stored overnight at -20°C for later microscopy evaluation.

4.3 Automated image acquisition and cell counting

The filters were evaluated microscopically under a Zeiss Axio Imager.Z2 stand (Carl Zeiss MicroImaging GmbH, Jena, Germany), equipped with a multipurpose fully automated microscope imaging system (MPISYS), a Colibri LED light source illumination system, and a multi-filter set 62HE (Carl Zeiss MicroImaging GmbH, Jena, Germany). Pictures were taken via a cooled charged-coupled-device (CCD) camera (AxioCam MRm; Carl Zeiss AG, Oberkochen, Germany) with a 63x oil objective, a numerical aperture of 1.4, and a pixel size of 0.1016 µm/pixel, coupled to the AxioVision SE64 Rel.4.9.1 software (Carl Zeiss AG, Oberkochen, Germany) as described by (Bennke et al., 2016). Exposure times were adjusted after manual inspection with the AxioVision

Rel.4.8 software coupled to the SamLoc 1.7 software (Zeder et al., 2011), which was also used to define the coordinates of the filters on the slides. For image acquisition, channels were defined with the MPISYS software, and a minimum of 55 fields of view with a minimum distance of 0.25 mm were acquired of each filter piece by recoding a z-stack of 7 images in autofocus.

Cell enumeration was performed with the software Automated Cell Measuring and Enumeration Tool (ACMETool3, 2018-11-09; M. Zeder, Technobiology GmbH, Buchrain, Switzerland). Cells were counted as objects according to manually defined parameters separately for the DAPI and FISH channels.

4.4 Calculation of consumed inorganic nutrients

Following (Fadeev et al., 2018) the nutrient consumption (Δ) at each station was calculated by subtracting the mean value of all collected measurements above 50 m from the mean value of all collected measurements between 50 and 100 m (below the seasonal pycnocline).

4.5 Statistical analyses

All statistical analyses and calculations in this study were performed using R (v3.6.3) (www.r-project.org) in RStudio (v1.2.5042). Statistical tests for normality, ANOVA and Kruskal-Wallis were conducted using the R software, post-hoc Wilcoxon test and Pearson's rank correlation coefficient were obtained with the R package "rstatix" (v0.5.0) (Kassambara, 2019). Plots were generated using the R package "ggplot2" (v3.3.0) (Wickham, 2016) and "tidyverse" (v1.3.0) (Wickham et al., 2019).

4.6 Data availability

All data is accessible via the Data Publisher for Earth & Environmental Science PANGAEA (www.pangaea.de): cell abundances under doi:10.1594/PANGAEA.905212, inorganic nutrient measurements under doi:10.1594/PANGAEA.906132. Scripts for processing the data can be accessed at https://github.com/edfadeev/FramStrait-counts.

4.7 Conflict of Interest

The authors declare that the research was conducted in the absence of any commercial or financial relationships that could be construed as a potential conflict of interest.

5 Author contributions

MC, EF and VS-C designed and conducted the study. MC, EF and VS-C wrote the manuscript with guidance from AB. All authors critically revised the manuscript and gave their approval of the submitted version.

6 Funding

This project has received funding from the European Research Council (ERC) under the European Union's Seventh Framework Program (FP7/2007-2013) research project ABYSS (Grant Agreement No. 294757) to AB. Additional funding came from the Helmholtz Association, specifically for the FRAM infrastructure, from the Max Planck Society and from the Hector Fellow Academy. This publication is Eprint ID 51358 of the Alfred Wegener Institute Helmholtz Center for Polar and Marine Research, Bremerhaven, Germany.

7 Acknowledgements

We thank the captain and crew of RV Polarstern expedition PS99.2, as well as the chief scientist Thomas Soltwedel for support with work at sea. We also thank Pier Offre for assistance in sampling, Greta Reintjes for designing the probe Opi346, Mareike Bach for technical support, Sinhue Torres-Valdes and Laura Wischnewski for conducting the inorganic nutrient measurements. We thank Andreas Ellrott for the support with the automated microscope from the Max Planck Institute for Marine Microbiology. This work was conducted in the framework of the HGF Infrastructure Program FRAM of the Alfred-Wegener-Institute Helmholtz Center for Polar and Marine.

8 References

Agogué, H., Lamy, D., Neal, P. R., Sogin, M. L., and Herndl, G. J. (2011). Water mass-specificity of bacterial communities in the North Atlantic revealed by massively parallel sequencing. *Mol. Ecol.* 20, 258–274. doi:10.1111/j.1365-294X.2010.04932.x.

Alonso-Saez, L., Waller, A. S., Mende, D. R., Bakker, K., Farnelid, H., Yager, P. L., et al. (2012). Role for urea in nitrification by polar marine Archaea. *Proc. Natl. Acad. Sci.* 109, 17989–17994. doi:10.1073/pnas.1201914109.

Amann, R. I., Binder, B. J., Olson, R. J., Chisholm, S. W., Devereux, R., and Stahl, D. A. (1990). Combination of 16S rRNA-targeted oligonucleotide probes with flow cytometry for analyzing mixed microbial populations. *Appl. Environ. Microbiol.* 56, 1919 LP – 1925.

Amano-Sato, C., Akiyama, S., Uchida, M., Shimada, K., and Utsumi, M. (2013). Archaeal distribution and abundance in water masses of the Arctic Ocean, Pacific sector. *Aquat. Microb. Ecol.* 69, 101–112.

Basedow, S. L., Sundfjord, A., von Appen, W. J., Halvorsen, E., Kwasniewski, S., and Reigstad, M. (2018). Seasonal variation in transport of Zooplankton Into the Arctic basin through the Atlantic Gateway, Fram Strait. *Front. Mar. Sci.* 5, 1–22. doi:10.3389/fmars.2018.00194.

Bennke, C. M., Reintjes, G., Schattenhofer, M., Ellrott, A., Wulf, J., Zeder, M., et al. (2016). Modification of a High-Throughput Automatic Microbial Cell Enumeration System for Shipboard Analyses. *Appl. Environ. Microbiol.* 82, 3289 LP – 3296. doi:10.1128/AEM.03931-15.

Beszczynska-Möller, A., Fahrbach, E., Schauer, U., and Hansen, E. (2012). Variability in Atlantic water temperature and transport at the entrance to the Arctic Ocean, 1997–2010. *ICES J. Mar. Sci.* 69, 852–863. doi:10.1093/icesjms/fss056.

Beszczynska-Möller, A., Woodgate, R., Lee, C., Melling, H., and Karcher, M. (2011). A Synthesis of Exchanges Through the Main Oceanic Gateways to the Arctic Ocean. *Oceanography* 24, 82–99. doi:10.5670/oceanog.2011.59.

Bižić-Ionescu, M., Zeder, M., Ionescu, D., Orlić, S., Fuchs, B. M., Grossart, H. P., et al. (2015). Comparison of bacterial communities on limnic versus coastal marine particles reveals profound differences in colonization. *Environ. Microbiol.* 17, 3500–3514. doi:10.1111/1462-2920.12466.

Boetius, A., Albrecht, S., Bakker, K., Bienhold, C., Felden, J., Fernandez-Mendez, M., et al. (2013).

Export of Algal Biomass from the Melting Arctic Sea Ice. *Science (80-.).* 339, 1430–1432. doi:10.1126/science.1231346.

Bowman, J. S., Rasmussen, S., Blom, N., Deming, J. W., Rysgaard, S., and Sicheritz-Ponten, T. (2012). Microbial community structure of Arctic multiyear sea ice and surface seawater by 454 sequencing of the 16S RNA gene. *ISME J.* 6, 11–20. doi:10.1038/ismej.2011.76.

Buchan, A., LeCleir, G. R., Gulvik, C. a., González, J. M., and Gonzalez, J. M. (2014). Master recyclers: features and functions of bacteria associated with phytoplankton blooms. *Nat. Rev. Microbiol.* 12, 686–698. doi:10.1038/nrmicro3326.

Cardman, Z., Arnosti, C., Durbin, A., Ziervogel, K., Cox, C., Steen, A. D., et al. (2014). Verrucomicrobia Are Candidates for Polysaccharide-Degrading Bacterioplankton in an Arctic Fjord of Svalbard. *Appl. Environ. Microbiol.* 80, 3749–3756. doi:10.1128/AEM.00899-14.

Church, M. J., DeLong, E. F., Ducklow, H. W., Karner, M. B., Preston, C. M., and Karl, D. M. (2003). Abundance and distribution of planktonic Archaea and Bacteria in the waters west of the Antarctic Peninsula. *Limnol. Oceanogr.* 48, 1893–1902. doi:10.4319/lo.2003.48.5.1893.

Colatriano, D., Tran, P. Q., Guéguen, C., Williams, W. J., Lovejoy, C., and Walsh, D. A. (2018). Genomic evidence for the degradation of terrestrial organic matter by pelagic Arctic Ocean Chloroflexi bacteria. *Commun. Biol.* 1, 90. doi:10.1038/s42003-018-0086-7.

Cottier, F., Tverberg, V., Inall, M., Svendsen, H., Nilsen, F., and Griffiths, C. (2005). Water mass modification in an Arctic fjord through cross-shelf exchange: The seasonal hydrography of Kongsfjorden, Svalbard. *J. Geophys. Res. Ocean.* 110, 1–18. doi:10.1029/2004JC002757.

Dai, A., Luo, D., Song, M., and Liu, J. (2019). Arctic amplification is caused by sea-ice loss under increasing CO2. *Nat. Commun.* 10, 121. doi:10.1038/s41467-018-07954-9.

de Steur, L., Hansen, E., Gerdes, R., Karcher, M., Fahrbach, E., and Holfort, J. (2009). Freshwater fluxes in the East Greenland Current: A decade of observations. *Geophys. Res. Lett.* 36, L23611. doi:10.1029/2009GL041278.

DeLong, E. F., Taylor, L. T., Marsh, T. L., and Preston, C. M. (1999). Visualization and Enumeration of Marine Planktonic Archaea and Bacteria by Using Polyribonucleotide Probes and Fluorescent In Situ Hybridization. *Appl. Environ. Microbiol.* 65, 5554 LP – 5563.

Dobal-Amador, V., Nieto-Cid, M., Guerrero-Feijoo, E., Hernando-Morales, V., Teira, E., and Varela, M. M. (2016). Vertical stratification of bacterial communities driven by multiple environmental factors in the waters (0–5000m) off the Galician coast (NW Iberian margin). *Deep Sea Res. Part I Oceanogr. Res. Pap.* 114, 1–11. doi:https://doi.org/10.1016/j.dsr.2016.04.009.

Dobricic, S., Vignati, E., and Russo, S. (2016). Large-Scale Atmospheric Warming in Winter and the Arctic Sea Ice Retreat. *J. Clim.* 29, 2869–2888. doi:10.1175/JCLI-D-15-0417.1.

Engel, A., Bracher, A., Dinter, T., Endres, S., Grosse, J., Metfies, K., et al. (2019). Inter-Annual Variability of Organic Carbon Concentration in the Eastern Fram Strait During Summer (2009–2017). *Front. Mar. Sci.* 6, 1–17. doi:10.3389/fmars.2019.00187.

Engel, A., Piontek, J., Metfies, K., Endres, S., Sprong, P., Peeken, I., et al. (2017). Inter-annual variability of transparent exopolymer particles in the Arctic Ocean reveals high sensitivity to ecosystem changes. *Sci. Rep.* 7, 4129. doi:10.1038/s41598-017-04106-9.

Fadeev, E., Salter, I., Schourup-Kristensen, V., Nöthig, E.-M., Metfies, K., Engel, A., et al. (2018). Microbial Communities in the East and West Fram Strait During Sea Ice Melting Season. *Front. Mar. Sci.* 5, 429. doi:10.3389/fmars.2018.00429.

Fernández-Méndez, M., Wenzhöfer, F., Peeken, I., Sørensen, H. L., Glud, R. N., and Boetius, A. (2014). Composition, buoyancy regulation and fate of ice algal aggregates in the Central Arctic Ocean. *PLoS One* 9, e107452–e107452. doi:10.1371/journal.pone.0107452.

Galand, P. E., Casamayor, E. O., Kirchman, D. L., and Lovejoy, C. (2009a). Ecology of the rare microbial biosphere of the Arctic Ocean. *Proc. Natl. Acad. Sci.* 106, 22427–22432. doi:10.1073/pnas.0908284106.

Galand, P. E., Casamayor, E. O., Kirchman, D. L., Potvin, M., and Lovejoy, C. (2009b). Unique archaeal assemblages in the Arctic Ocean unveiled by massively parallel tag sequencing. *ISME J.* 3, 860–869. doi:10.1038/ismej.2009.85.

Galand, P. E., Potvin, M., Casamayor, E. O., and Lovejoy, C. (2010). Hydrography shapes bacterial biogeography of the deep Arctic Ocean. *ISME J.* 4, 564–576. doi:10.1038/ismej.2009.134.

Giebel, H. A., Kalhoefer, D., Lemke, A., Thole, S., Gahl-Janssen, R., Simon, M., et al. (2011). Distribution of Roseobacter RCA and SAR11 lineages in the North Sea and characteristics of an abundant RCA isolate. *ISME J.* 5, 8–19. doi:10.1038/ismej.2010.87.

Giovannoni, S. J. (2017). SAR11 Bacteria: The Most Abundant Plankton in the Oceans. *Ann. Rev. Mar. Sci.* 9, 231–255. doi:10.1146/annurev-marine-010814-015934.

Gloor, G. B., Macklaim, J. M., Pawlowsky-Glahn, V., and Egozcue, J. J. (2017). Microbiome Datasets Are Compositional: And This Is Not Optional . *Front. Microbiol.* 8, 2224.

Hebbeln, D., and Wefer, G. (1991). Effects of ice coverage and ice-rafted material on sedimentation in the Fram Strait. *Nature* 350, 409–411. doi:10.1038/350409a0.

Herndl, G. J., Reinthaler, T., Teira, E., van Aken, H., Veth, C., Pernthaler, A., et al. (2005). Contribution of Archaea to Total Prokaryotic Production in the Deep Atlantic Ocean. *Appl. Environ. Microbiol.* 71, 2303–2309. doi:10.1128/AEM.71.5.2303-2309.2005.

Hewson, I., Steele, J. A., Capone, D. G., and Fuhrman, J. A. (2006). Remarkable heterogeneity in meso- and bathypelagic bacterioplankton assemblage composition. *Limnol. Oceanogr.* 51, 1274–1283. doi:10.4319/lo.2006.51.3.1274.

Joint, I., Henriksen, P., Fonnes, G., Bourne, D., Thingstad, T., and Riemann, B. (2002). Competition for inorganic nutrients between phytoplankton and bacterioplankton in nutrient manipulated mesocosms. *Aquat. Microb. Ecol.* 29, 145–159. doi:10.3354/ame029145.

Karner, M. B., DeLong, E. F., and Karl, D. M. (2001). Archaeal dominance in the mesopelagic zone of the Pacific Ocean. *Nature* 409, 507–510. doi:10.1038/35054051.

Kassambara, A. (2019). rstatix: Pipe-Friendly Framework for Basic Statistical Tests.

Kirchman, D. L., Elifantz, H., Dittel, A. I., Malmstrom, R. R., and Cottrell, M. T. (2007). Standing stocks and activity of Archaea and Bacteria in the western Arctic Ocean. *Limnol. Oceanogr.* 52, 495–507. doi:10.4319/lo.2007.52.2.0495.

Korhonen, M., Rudels, B., Marnela, M., Wisotzki, A., and Zhao, J. (2013). Time and space variability of freshwater content, heat content and seasonal ice melt in the Arctic Ocean from 1991 to 2011. *Ocean Sci.* 9, 1015–1055. doi:10.5194/os-9-1015-2013.

Kraemer, S., Ramachandran, A., Colatriano, D., Lovejoy, C., and Walsh, D. A. (2020). Diversity and biogeography of SAR11 bacteria from the Arctic Ocean. *ISME J.* 14, 79–90. doi:10.1038/s41396-019-0499-4.

Kumar, M. S., Slud, E. V, Okrah, K., Hicks, S. C., Hannenhalli, S., and Bravo, H. C. (2018). Analysis and correction of compositional bias in sparse sequencing count data. *BMC Genomics* 19, 799.

Landry, Z., Swan, B. K., Herndl, G. J., Stepanauskas, R., and Giovannoni, S. J. (2017). SAR202 Genomes from the Dark Ocean Predict Pathways for the Oxidation of Recalcitrant Dissolved Organic Matter. *MBio* 8, e00413--17. doi:10.1128/mBio.00413-17.

Leu, E., Søreide, J. E., Hessen, D. O., Falk-Petersen, S., and Berge, J. (2011). Consequences of changing sea-ice cover for primary and secondary producers in the European Arctic shelf seas: Timing, quantity, and quality. *Prog. Oceanogr.* 90, 18–32. doi:10.1016/j.pocean.2011.02.004.

Luo, H., and Moran, M. A. (2014). Evolutionary Ecology of the Marine Roseobacter Clade. *Microbiol. Mol. Biol. Rev.* 78, 573–587. doi:10.1128/MMBR.00020-14.

Müller, O., Seuthe, L., Bratbak, G., and Paulsen, M. L. (2018a). Bacterial Response to Permafrost Derived Organic Matter Input in an Arctic Fjord. *Front. Mar. Sci.* 5. doi:10.3389/fmars.2018.00263.

Müller, O., Wilson, B., Paulsen, M. L., Rumińska, A., Armo, H. R., Bratbak, G., et al. (2018b). Spatiotemporal Dynamics of Ammonia-Oxidizing Thaumarchaeota in Distinct Arctic Water Masses. *Front. Microbiol.* 9, 1–13. doi:10.3389/fmicb.2018.00024.

Mundy, C. J., Barber, D. G., and Michel, C. (2005). Variability of snow and ice thermal, physical and optical properties pertinent to sea ice algae biomass during spring. *J. Mar. Syst.* 58, 107–120.

Nöthig, E.-M., Bracher, A., Engel, A., Metfies, K., Niehoff, B., Peeken, I., et al. (2015). Summertime plankton ecology in Fram Strait—a compilation of long- and short-term observations. *Polar Res.* 34, 23349. doi:10.3402/polar.v34.23349.

Nöthig, E.-M., Petersen, I., Schröter, F., and Lorenzen, C. (2018). "Chlorophyll a measured on water bottle samples during POLARSTERN cruise PS94 (ARK-XXIX/3)," in *Lorenzen, Christiane; Lalande, Catherine; Knüppel, Nadine; Winkler, Maria; Bonk, Elizabeth; Strache, Anique; Jacobs, Mirta; Petersen, Imke; Schröter, Franz* (PANGAEA). doi:10.1594/PANGAEA.887934.

Peng, G., and Meier, W. N. (2018). Temporal and regional variability of Arctic sea-ice coverage

from satellite data. *Ann. Glaciol.* 59, 191–200. doi:10.1017/aog.2017.32.

Pernthaler, A., Pernthaler, J., and Amann, R. (2002). Fluorescence In Situ Hybridization and Catalyzed Reporter Deposition for the Identification of Marine Bacteria. *Appl. Environ. Microbiol.* 68, 3094 LP – 3101. doi:10.1128/AEM.68.6.3094-3101.2002.

Perrette, M., Yool, A., Quartly, G. D., and Popova, E. E. (2011). Near-ubiquity of ice-edge blooms in the Arctic. *Biogeosciences* 8, 515–524. doi:10.5194/bg-8-515-2011.

Piontek, J., Sperling, M., Nöthig, E.-M., and Engel, A. (2014). Regulation of bacterioplankton activity in Fram Strait (Arctic Ocean) during early summer: The role of organic matter supply and temperature. *J. Mar. Syst.* 132, 83–94. doi:10.1016/j.jmarsys.2014.01.003.

Piontek, J., Sperling, M., Nöthig, E.-M., and Engel, A. (2015). Multiple environmental changes induce interactive effects on bacterial degradation activity in the Arctic Ocean. *Limnol. Oceanogr.* 60, 1392–1410. doi:10.1002/lno.10112.

Piwosz, K., Shabarova, T., Pernthaler, J., Posch, T., Šimek, K., Porcal, P., et al. (2020). Bacterial and Eukaryotic Small-Subunit Amplicon Data Do Not Provide a Quantitative Picture of Microbial Communities, but They Are Reliable in the Context of Ecological Interpretations. *mSphere* 5, 1–14. doi:10.1128/mSphere.00052-20.

Polyakov, I. V., Pnyushkov, A. V., Alkire, M. B., Ashik, I. M., Baumann, T. M., Carmack, E. C., et al. (2017). Greater role for Atlantic inflows on sea-ice loss in the Eurasian Basin of the Arctic Ocean. *Science (80-.).* 356, 285–291. doi:10.1126/science.aai8204.

Quast, C., Pruesse, E., Yilmaz, P., Gerken, J., Schweer, T., Yarza, P., et al. (2012). The SILVA ribosomal RNA gene database project: improved data processing and web-based tools. *Nucleic Acids Res.* 41, D590–D596. doi:10.1093/nar/gks1219.

Quero, G. M., Celussi, M., Relitti, F., Kovačević, V., Del Negro, P., and Luna, G. M. (2019). Inorganic and Organic Carbon Uptake Processes and Their Connection to Microbial Diversity in Meso- and Bathypelagic Arctic Waters (Eastern Fram Strait). *Microb. Ecol.* doi:10.1007/s00248-019-01451-2.

Rudels, B., Schauer, U., Björk, G., Korhonen, M., Pisarev, S., Rabe, B., et al. (2013). Observations of water masses and circulation in the Eurasian Basin of the Arctic Ocean from the 1990s to the late 2000s. *OS Spec. Issue Ice-Atmosphere-Ocean Interact. Arct. Ocean Dur. IPY Damocles Proj.* 9, 147–169.

Salazar, G., Cornejo-Castillo, F. M., Benítez-Barrios, V., Fraile-Nuez, E., Álvarez-Salgado, X. A., Duarte, C. M., et al. (2016). Global diversity and biogeography of deep-sea pelagic prokaryotes. *ISME J.* 10, 596–608. doi:10.1038/ismej.2015.137.

Saw, J. H. W., Nunoura, T., Hirai, M., Takaki, Y., Parsons, R., Michelsen, M., et al. (2020). Pangenomics Analysis Reveals Diversification of Enzyme Families and Niche Specialization in Globally Abundant SAR202 Bacteria. *MBio* 11.

Schattenhofer, M., Fuchs, B. M., Amann, R., Zubkov, M. V, Tarran, G. A., and Pernthaler, J. (2009). Latitudinal distribution of prokaryotic picoplankton populations in the Atlantic Ocean. 1–16.

doi:10.1111/j.1462-2920.2009.01929.x.

Selje, N., Simon, M., and Brinkhoff, T. (2004). A newly discovered Roseobacter cluster in temperate and polar oceans. *Nature* 427, 445–448. doi:10.1038/nature02272.

Sheik, C. S., Jain, S., and Dick, G. J. (2014). Metabolic flexibility of enigmatic SAR 324 revealed through metagenomics and metatranscriptomics. *Environ. Microbiol.* 16, 304–317.

Sogin, M. L., Morrison, H. G., Huber, J. A., Welch, D. M., Huse, S. M., Neal, P. R., et al. (2006). Microbial diversity in the deep sea and the underexplored "rare biosphere." *Proc. Natl. Acad. Sci.* 103, 12115–12120.

Soltwedel, T., Bauerfeind, E., Bergmann, M., Bracher, A., Budaeva, N., Busch, K., et al. (2016). Natural variability or anthropogenically-induced variation? Insights from 15 years of multidisciplinary observations at the arctic marine LTER site HAUSGARTEN. *Ecol. Indic.* 65, 89–102.

Soltwedel, T., Bauerfeind, E., Bergmann, M., Budaeva, N., Hoste, E., Jaeckisch, N., et al. (2005). HAUSGARTEN: multidisciplinary investigations at a deep-sea, long-term observatory in the Arctic Ocean. *Oceanography*.

Sperling, M., Giebel, H. A., Rink, B., Grayek, S., Staneva, J., Stanev, E., et al. (2012). Differential effects of hydrographic and biogeochemical properties on the SAR11 clade and Roseobacter RCA cluster in the North Sea. *Aquat. Microb. Ecol.* 67, 25–34. doi:10.3354/ame01580.

Sun, L., Perlwitz, J., and Hoerling, M. (2016). What caused the recent "Warm Arctic, Cold Continents" trend pattern in winter temperatures? *Geophys. Res. Lett.* 43, 5345–5352. doi:10.1002/2016GL069024.

Swan, B. K., Martinez-Garcia, M., Preston, C. M., Sczyrba, A., Woyke, T., Lamy, D., et al. (2011). Potential for Chemolithoautotrophy Among Ubiquitous Bacteria Lineages in the Dark Ocean. *Science (80-.).* 333, 1296–1300. doi:10.1126/science.1203690.

Tada, Y., Makabe, R., Kasamatsu-Takazawa, N., Taniguchi, A., and Hamasaki, K. (2013). Growth and distribution patterns of Roseobacter/Rhodobacter, SAR11, and Bacteroidetes lineages in the Southern Ocean. *Polar Biol.* 36, 691–704. doi:10.1007/s00300-013-1294-8.

Tada, Y., Taniguchi, A., Nagao, I., Miki, T., Uematsu, M., Tsuda, A., et al. (2011). Differing Growth Responses of Major Phylogenetic Groups of Marine Bacteria to Natural Phytoplankton Blooms in the Western North Pacific Ocean. 77, 4055–4065. doi:10.1128/AEM.02952-10.

Teeling, H., Fuchs, B. M., Becher, D., Klockow, C., Gardebrecht, A., Bennke, C. M., et al. (2012). Substrate-controlled succession of marine bacterioplankton populations induced by a phytoplankton bloom. *Science (80-.).* 336, 608–611.

Teeling, H., Fuchs, B. M., Bennke, C. M., Krueger, K., Chafee, M., Kappelmann, L., et al. (2016). Recurring patterns in bacterioplankton dynamics during coastal spring algae blooms. *Elife* 5, e11888.

Teira, E., Lebaron, P., Van Aken, H., and Herndl, G. J. (2006). Distribution and activity of Bacteria

and Archaea in the deep water masses of the North Atlantic. *Limnol. Oceanogr.* 51, 2131–2144.

Teira, E., Reinthaler, T., Pernthaler, A., Pernthaler, J., and Herndl, G. J. (2004). Combining catalyzed reporter deposition-fluorescence in situ hybridization and microautoradiography to detect substrate utilization by bacteria and archaea in the deep ocean. *Appl. Environ. Microbiol.* 70, 4411–4414.

Tippenhauer, S., Torres-Valdes, S., Fong, A. A., Krauß, F., Huchler, M., and Wisotzki, A. (2017). Physical oceanography measured on water bottle samples during POLARSTERN cruise PS99.2 (ARK-XXX/1.2). doi:10.1594/PANGAEA.871952.

Varela, M. M., Van Aken, H. M., and Herndl, G. J. (2008). Abundance and activity of Chloroflexi-type SAR202 bacterioplankton in the meso-and bathypelagic waters of the (sub) tropical Atlantic. *Environ. Microbiol.* 10, 1903–1911.

Vernet, M., Richardson, T. L., Metfies, K., Nöthig, E.-M., and Peeken, I. (2017). Models of Plankton Community Changes during a Warm Water Anomaly in Arctic Waters Show Altered Trophic Pathways with Minimal Changes in Carbon Export. *Front. Mar. Sci.* 4, 1–19. doi:10.3389/fmars.2017.00160.

von Appen, W.-J., Schauer, U., Somavilla, R., Bauerfeind, E., and Beszczynska-Möller, A. (2015). Exchange of warming deep waters across Fram Strait. *Deep Sea Res. Part I Oceanogr. Res. Pap.* 103, 86–100. doi:10.1016/j.dsr.2015.06.003.

Walczowski, W., Beszczynska-Möller, A., Wieczorek, P., Merchel, M., and Grynczel, A. (2017). Oceanographic observations in the Nordic Sea and Fram Strait in 2016 under the IO PAN long-term monitoring program AREX. *Oceanologia* 59, 187–194. doi:10.1016/j.oceano.2016.12.003.

Wassmann, P., and Reigstad, M. (2011). Future Arctic Ocean seasonal ice zones and implications for pelagic-benthic coupling. *Oceanography* 24, 220–231. doi:10.5670/oceanog.2011.74.

Wekerle, C., Wang, Q., von Appen, W.-J., Danilov, S., Schourup-Kristensen, V., and Jung, T. (2017). Eddy-Resolving Simulation of the Atlantic Water Circulation in the Fram Strait With Focus on the Seasonal Cycle. *J. Geophys. Res. Ocean.* 122, 8385–8405. doi:10.1002/2017JC012974.

Wells, L. E., Cordray, M., Bowerman, S., Miller, L. A., Vincent, W. F., and Deming, J. W. (2006). Archaea in particle-rich waters of the Beaufort Shelf and Franklin Bay, Canadian Arctic: Clues to an allochthonous origin? *Limnol. Oceanogr.* 51, 47–59.

Wells, L. E., and Deming, J. W. (2003). Abundance of bacteria, the Cytophaga-Flavobacterium cluster and Archaea in cold oligotrophic waters and nepheloid layers of the Northwest Passage, Canadian archipelago. *Aquat. Microb. Ecol.* 31, 19–31. doi:10.3354/ame031019.

Wickham, H. (2016). "Getting Started with ggplot2," in *ggplot2* (Springer), 11–31.

Wickham, H., Averick, M., Bryan, J., Chang, W., McGowan, L., François, R., et al. (2019). Welcome to the Tidyverse. *J. Open Source Softw.* 4, 1686.

Wilson, B., Müller, O., Nordmann, E.-L., Seuthe, L., Bratbak, G., and Øvreås, L. (2017). Changes in

Marine Prokaryote Composition with Season and Depth Over an Arctic Polar Year. *Front. Mar. Sci.* 4. doi:10.3389/fmars.2017.00095.

Wilson, C., and Wallace, D. W. R. (1990). Using the Nutrient Ratio No Po As a Tracer of Continental-Shelf Waters in the Central Arctic-Ocean. *J. Geophys. Res.* 95, 22193–22208.

Zeder, M., Ellrott, A., and Amann, R. (2011). Automated sample area definition for high-throughput microscopy. *Cytom. Part A* 79, 306–310.

9 Figures and Tables

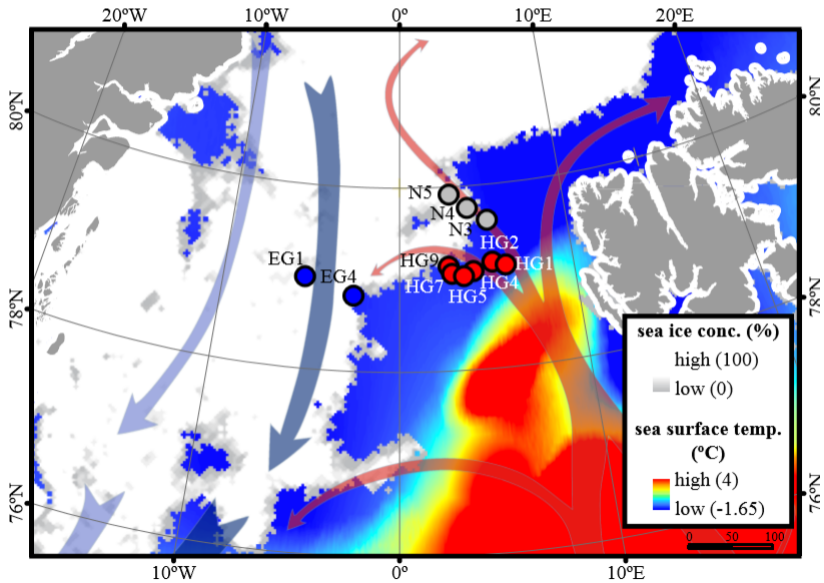

Figure 1. Oceanographic overview of the Fram Strait, including the monthly mean of sea-ice cover and sea surface temperature during July 2016. The sea ice concentration is represented by inverted grayscale (gray=low, white=high). Arrows represent general directions of the WSC (in red) and the EGC (in blue). Stations of water column sampling are indicated and colored according to their sea-ice conditions: ice-covered EGC stations - blue, marginal ice N stations - gray, ice-free WSC stations - red.

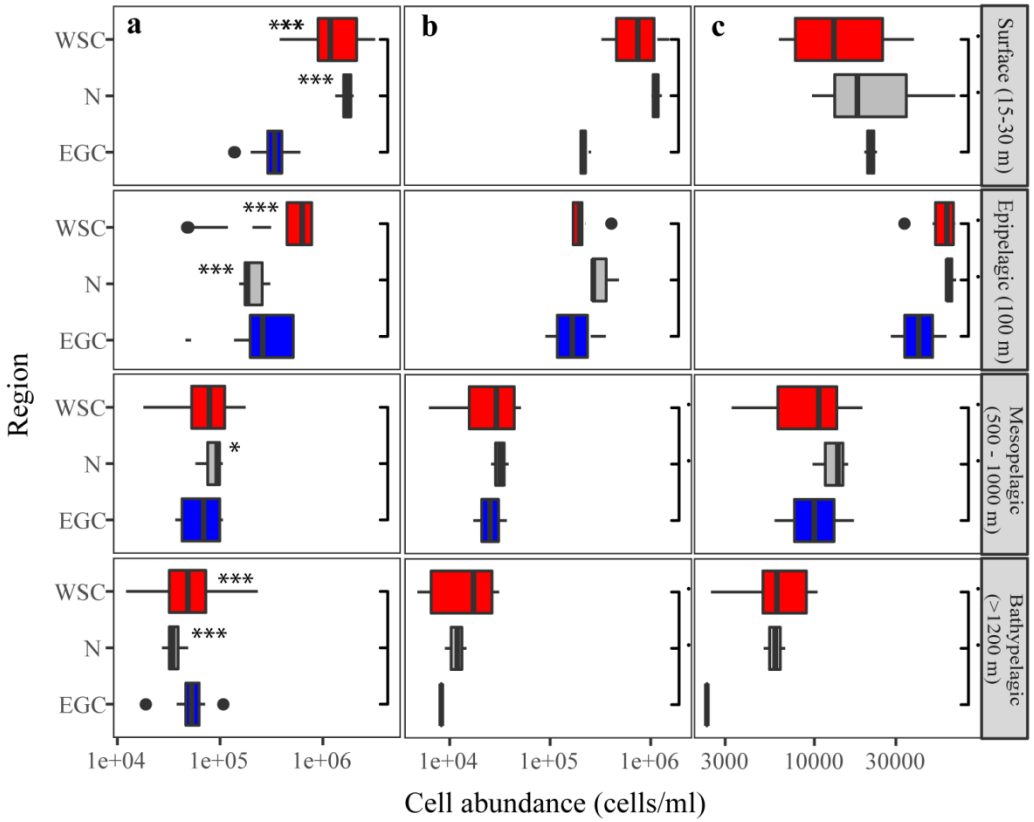

Figure 2. Bacterioplankton cell abundances in the different regions of the Fram Strait: Total bacterioplankton (A); *Bacteria* (B); and *Archaea* (C). Note the different scale of the cell abundances for *Archaea*. The different regions are indicated by color: ice-covered EGC- blue, marginal ice N - gray, ice-free WSC - red. The asterisks represent levels of statistical significance of difference between all three regions per depth and domain: * < 0.05, ** < 0.01, *** < 0.001.

Table 1. Average cell abundances and proportions (% of DAPI stained cells) of selected taxonomic groups in surface (0 – 30 m) and epipelagic (100 m) depths of different regions across the Fram Strait. The proportions (%) were calculated based on the total bacterioplankton cell abundances, 'n' represents the number of counted fields of view. All values are represented in 10^5 cells mL^{-1}. SAR11 clade (SAR11), *Gammaproteobacteria* (GAM), *Alteromonadaceae/Colwelliaceae/Pseudoalteromonadaceae* (ATL), *Bacteroidetes* (BACT), *Polaribacter* (POL), *Verrucomicrobiales* (VER), *Opitutales* (OPI), *Rhodobacteraceae* (ROS), *Deltaproteobacteria* (DELTA), and *Thaumarchaeota* (THA).

Region	**Water layer**	**SAR11**	**%**	**n**	**GAM**	**%**	**n**	**ALT**	**%**	**n**	**BACT**	**%**	**n**	**POL**	**%**	**n**
EGC	Surface	1.9 ± 0.7	49.6	53	0.3 ± 0.2	12.5	67	0.2 ± 0.1	7.3	64	0.6 ± 0.4	17.8	66	0.4 ± 0.3	11.1	62
EGC	Epipelagic	1.0 ± 0.6	26.2	50	0.2 ± 0.1	5.4	77	0.1 ± 0.0	2.3	61	0.3 ± 0.2	8.0	93	0.1 ± 0.0	2.3	52
N	Surface	4.2 ± 1.0	23.5	81	2.1 ± 0.6	12.8	78	0.1 ± 0.0	0.8	68	2.1 ± 0.8	12.2	85	1.3 ± 0.6	8.3	85
N	Epipelagic	2.2 ± 0.3	29.0	73	0.4 ± 0.1	4.7	109	0.2 ± 0.1	1.8	87	0.4 ± 0.1	6.0	102	0.1 ± 0.0	1.6	98
WSC	Surface	6.1 ± 2.0	38.3	150	1.6 ± 0.3	13.6	189	0.3 ± 0.1	2.4	186	2.1 ± 1.0	16.1	163	0.8 ± 0.2	6.6	162
WSC	Epipelagic	1.9 ± 0.2	32.1	175	0.2 ± 0.0	2.9	214	0.1 ± 0.0	1.3	186	0.2 ± 0.0	4.2	195	0.1 ± 0.0	1.4	176
Region	**Water layer**	**VER**	**%**	**n**	**OPI**	**%**	**n**	**ROS**	**%**	**n**	**DELTA**	**%**	**n**	**THA**	**%**	**n**
EGC	Surface	0.1 ± 0.0	2.5	41	0.1 ± 0.0	2.4	53	0.2 ± 0.1	7.0	44	0.2 ± 0.1	6.6	57	0.1 ± 0.0	2.9	34
EGC	Epipelagic	0.1 ± 0.0	1.8	63	0.1 ± 0.0	2.1	70	0.3 ± 0.2	9.0	60	0.1 ± 0.0	3.8	67	0.1 ± 0.02	3.9	75
N	Surface	0.9 ± 0. 1	5.2	91	0.9 ± 0.01	5.3	91	0.6 ± 0.0	3.1	92	0.2 ± 0.1	1.3	86	0.1 ± 0.0	05	65
N	Epipelagic	0.2 ± 0.1	1.9	98	0.2 ± 0.1	2.1	107	0.2 ± 0.0	2.7	108	0.2 ± 0.0	2.6	94	0.3 ± 0.0	4.2	122

WSC	Surface	1.1 ± 0.0	5.0	171	0.8 ± 0.3	5.3	172	0.7 ± 0.3	3.7	165	0.1 ± 0.0	1.2	121	0.1 ± 0.0	0.5	178
WSC	Epipelagic	0.1 ± 0.0	1.5	219	0.1 ± 0.0	1.8	238	0.1 ± 0.0	2.4	223	0.2 ± 0.1	3.7	196	0.3 ± 0.1	5.0	246

Table 2. Average cell abundances and proportions (% of DAPI stained cells) of selected taxonomic groups in deep water layers of the different regions across the Fram Strait. The proportions (%) were calculated based on the total bacterioplankton cell abundances, 'n' represents the number of counted fields of view. All values are represented in 10^5 cells mL^{-1}. *Chloroflexi* (CFX), *Deltaproteobacteria* (DELTA), *Thaumarchaeota* (THA), *Rhodobacteraceae* (ROS), SAR202, SAR324, SAR406 and SAR11 clades.

Region	Water layer	CFX	%	n	DELTA	%	n	THA	%	n	ROS	%	n
EGC	Mesopelagic	0.02 ± 0.0	4.5	57	0.03 ± 0.010	4.5	45	0.01 ± 0.0	1.6	27	0.1 ± 0.0	11.1	75
EGC	Bathypelagic	0.02 ± NA	3.9	18	0.02 ± NA	3.3	33	0.01 ± NA	2.1	14	0.03 ± NA	5.1	14
N	Mesopelagic	0.03 ± 0.0	3.0	116	0.04 ± 0.0	4.6	99	0.01 ± 0.0	1.4	28	0.1 ± 0.01	13.3	128
N	Bathypelagic	0.02 ± 0.0	5.8	115	0.03 ± 0.0	8.1	123	0.01 ± 0.0	3.5	39	0.1 ± 0.0	20	122
WSC	Mesopelagic	0.03 ± 0.0	3.2	217	0.1± 0.01	6.0	139	0.02 ± 0.0	2.6	86	0.1 ± 0.01	6.7	195
WSC	Bathypelagic	0.02 ± 0.0	4.4	199	0.1 ± 0.02	8.9	130	0.02 ± 0.0	3.9	54	0.04 ± 0.01	13.8	197
Region	**Water layer**	**SAR202**	**%**	**n**	**SAR324**	**%**	**n**	**SAR406**	**%**	**n**	**SAR11**	**%**	**n**
EGC	Mesopelagic	0.02 ± 0.0	4.2	55	0.05 ± 0.0	6.4	60	0.01 ± 0.0	1.36	11	0.15 ± 0.1	21.9	49
EGC	Bathypelagic	0.02 ± NA	5.4	26	0.03 ± NA	4.7	35	0.01 ± NA	2.69	6	0.07 ± NA	13.9	32
N	Mesopelagic	0.03 ± 0.0	3.1	107	0.06 ± 0.0	5.9	66	0.01 ± 0.0	1.21	18	0.17 ± 0.0	20.2	101
N	Bathypelagic	0.03 ± 0.0	7.7	120	0.03 ± 0.0	7.5	54	0.01 ± 0.0	3.48	37	0.09 ± 0.0	26.5	85

WSC	Mesopelagic	0.03 ± 0.0	4.5	215	0.05 ± 0.0	5.4	168	0.01 ± 0.0	2.13	37	0.16 ± 0.0	18.8	166
WSC	Bathypelagic	0.03 ± 0.0	7.1	210	0.05 ± 0.0	6.2	138	0.01 ± 0.0	3.05	45	0.09 ± 0.0	21.4	201